

## How do InAs quantum dots relax when the InAs growth thickness exceeds the dislocation-induced critical thickness?

J. F. Chen, Y. C. Lin, C. H. Chiang, Ross C. C. Chen, Y. F. Chen, Y. H. Wu, and L. Chang

Citation: [Journal of Applied Physics](#) **111**, 013709 (2012); doi: 10.1063/1.3675519

View online: <http://dx.doi.org/10.1063/1.3675519>

View Table of Contents: <http://scitation.aip.org/content/aip/journal/jap/111/1?ver=pdfcov>

Published by the [AIP Publishing](#)

---

### Articles you may be interested in

[Piezoelectric InAs \(211\)B quantum dots grown by molecular beam epitaxy: Structural and optical properties](#)  
J. Appl. Phys. **108**, 103525 (2010); 10.1063/1.3510490

[Presentation and experimental validation of a model for the effect of thermal annealing on the photoluminescence of self-assembled InAs/GaAs quantum dots](#)  
J. Appl. Phys. **107**, 123107 (2010); 10.1063/1.3431388

[Annealing of self-assembled InAs/GaAs quantum dots: A stabilizing effect of beryllium doping](#)  
Appl. Phys. Lett. **94**, 072105 (2009); 10.1063/1.3086298

[Dislocation-induced spatial ordering of InAs quantum dots: Effects on optical properties](#)  
J. Appl. Phys. **91**, 5826 (2002); 10.1063/1.1467963

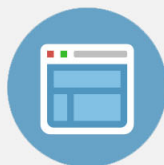
[Strain-induced material intermixing of InAs quantum dots in GaAs](#)  
Appl. Phys. Lett. **77**, 1789 (2000); 10.1063/1.1311314

---



## Re-register for Table of Content Alerts

Create a profile.



Sign up today!



## How do InAs quantum dots relax when the InAs growth thickness exceeds the dislocation-induced critical thickness?

J. F. Chen,<sup>1,a)</sup> Y. C. Lin,<sup>1</sup> C. H. Chiang,<sup>1</sup> Ross C. C. Chen,<sup>1</sup> Y. F. Chen,<sup>1</sup> Y. H. Wu,<sup>2</sup>  
and L. Chang<sup>2</sup>

<sup>1</sup>*Department of Electrophysics, National Chiao Tung University, Hsinchu, Taiwan 30050*

<sup>2</sup>*Department of Materials Science and Engineering, National Chiao Tung University, Hsinchu, Taiwan 30050*

(Received 4 June 2011; accepted 9 December 2011; published online 9 January 2012)

A simple critical thickness for generating lattice misfits is insufficient to describe the onset strain relaxation in InAs quantum dots (QDs). A predominant dot family is shown to relieve its strain by In/Ga interdiffusion, rather than by lattice misfits, at the onset of strain relaxation. This argument is based on photoluminescence spectra, which show the emergence of a fine blueshifted transition at the onset of strain relaxation, along with a low-energy transition from a dot family degraded by lattice misfits. From the analysis of the temperature-dependent blueshift and energy separation between the ground and excited-state transitions, the blueshift is attributed to In/Ga interdiffusion. Transmission electron microscopy suggests a relaxation-induced indium migration from the interdiffused dot family to the dislocated dot family. Post-growth thermal annealing can further relieve strain by inducing more In/Ga interdiffusion in the interdiffused dot family and more dislocations in the dislocated dot family. This study explains the co-existence of strong carrier confinement in the QDs and enormous misfit-related traps in the capacitance-voltage spectra, and an elongated QD electron-emission time. © 2012 American Institute of Physics.

[doi:[10.1063/1.3675519](https://doi.org/10.1063/1.3675519)]

### I. INTRODUCTION

When the InAs deposition thickness exceeds a critical thickness, compressive strain in InAs self-assembled quantum dots (QDs)<sup>1–15</sup> is relaxed and lattice misfits near the QDs and threading dislocations in the top GaAs layer are observed.<sup>16,17</sup> Relaxation in this way is undesirable because the induced defects severely degrade the photoluminescence (PL) spectra of the QDs. By capping the QDs with an InGaAs strain-relieving layer and carefully controlling the InAs growth thickness, the threading dislocations in the GaAs layer can be avoided and the relaxation does not severely degrade the PL spectra. The PL spectra of the QDs exhibit an abnormal PL blueshift at the onset of strain relaxation.<sup>18,19</sup> The capacitance-voltage (C-V) spectra revealed the confusing co-existence of strong electron confinement in the QD layer and enormous misfit-related traps at about 0.35 eV.<sup>20</sup> Electron emission time from the QDs is significantly elongated, compared to that from the coherent QDs before relaxation.<sup>20</sup> These observations cannot be explained by a simple compressive strain relaxation by lattice misfits, which is expected to decrease the bandgap of the QDs and cause a redshift. An understanding of the detailed mechanisms of the onset strain relaxation is necessary in order to tailor the properties of the QDs.

When the InAs growth thickness is increased, due to size fluctuation certain QDs are larger than others and the first strain is relieved by lattice misfits. The long range strain field due to these structural imperfections can affect the kinetics of adatom migrations.<sup>21,22</sup> It has been reported that defects such

as dislocations can be energetically favorable sites for indium migration.<sup>18,23</sup> Given sufficient kinetics, the dislocated QDs might affect the strain relieving process of the nearby not yet relaxed QDs. This suggests a more complicated strain relaxation process in the QDs. To study the mechanism of onset strain relaxation, we minutely increased the InAs growth thickness to exceed the dislocation-induced critical thickness with a main purpose to establish the origin of the abnormal blueshift. We showed a degraded PL transition in concomitance with the emergence of a blueshifted transition at the onset of strain relaxation. Increasing the InAs growth thickness could increase the blueshift. From analyzing the energy separation and the temperature dependence of the blueshifted PL spectra, this blueshift is attributed to In/Ga interdiffusion. Hence, a predominant dot family is strain relaxed by In/Ga interdiffusion, in addition to another dot family relaxed by lattice misfits. Cross-sectional transmission electron microscopy (TEM) images show a predominant dot family with truncated trapezium shape, as observed in coherent QDs before relaxation, and another family of large dislocated dots. Post-growth thermal annealing produces opposite wavelength shifts in the PL spectra of these two dot families, suggesting different strain relaxation processes.

### II. EXPERIMENT

The InAs dots were grown by solid source molecular beam epitaxy on top of a n<sup>+</sup>-GaAs (100) substrate, a 0.3 μm-thick Si-doped GaAs ( $\sim 7 \times 10^{16} \text{ cm}^{-3}$ ) barrier layer. The QD layer was realized by depositing an InAs layer from 1.97 to 3.3 monolayer (ML) at 490 °C (at a rate of 0.26 Å/s). After that, a 60 Å In<sub>0.15</sub>Ga<sub>0.85</sub>As capping layer was grown at 490 °C, followed by the growth of a low temperature GaAs

<sup>a)</sup>Author to whom correspondence should be addressed. Electronic mail: [jfchen@cc.nctu.edu.tw](mailto:jfchen@cc.nctu.edu.tw).

layer for 20 s at 490 °C. Then, the growth was interrupted for 3 min to ramp temperature to 600 °C for the growth of a 0.2  $\mu\text{m}$ -thick Si-doped GaAs barrier layer to terminate the growth procedure. The dot sheet density was estimated to be about  $3 \times 10^{10} \text{ cm}^{-2}$ . For C-V and deep-level transient spectroscopy (DLTS) probing, Schottky diodes were realized by evaporating Al with an area of  $5 \times 10^{-3} \text{ cm}^2$ .

### III. MEASUREMENT AND RESULTS

#### A. Effect of onset strain relaxation on the PL spectra

Figures 1(a) and 1(b) show the 50 and 300 K PL spectra of the InAs QDs with different InAs growth thicknesses. When the InAs thickness is increased from 1.97 to 2.7 ML, the spectra display a ground-state dominated transition from a uniform dot family with an expected redshift due to dot size increase. With the InGaAs capping layer to retard In/Ga interdiffusion, this redshift saturates at  $\sim 1300 \text{ nm}$  at 300 K (1250 nm at 50 K) with improved uniformity as seen in the 2.7 ML case. These QDs are coherently strained without detectable defects. However, with increasing the InAs thickness to 2.93 ML, the  $\sim 1300 \text{ nm}$  transition drastically reduces its intensity, suggesting generation of dislocations, consistent with the observation of a misfit-related trap at about 0.35 eV by DLTS<sup>20</sup> and lattice misfits by TEM pictures near the QD layer. Thus, the dislocation-induced critical thickness is between 2.7 and 2.93 ML. Increasing the InAs thickness to 3.06 and 3.3 ML further degrades this 1300 nm transition. When the temperature is lowered from 300 to 50 K, its peak intensity improves by only a factor of about two, suggesting a detrimental effect of non-radioactive defects through which photo-generated carriers are recombined. This feature suggests that the related dot family is degraded by lattice misfits and is denoted by dislocated QDs.

Besides this degraded transition, the PL spectra in Fig. 1 show another transition with an abnormal blueshift from 50 to 70 meV with increasing the InAs thickness at the onset of

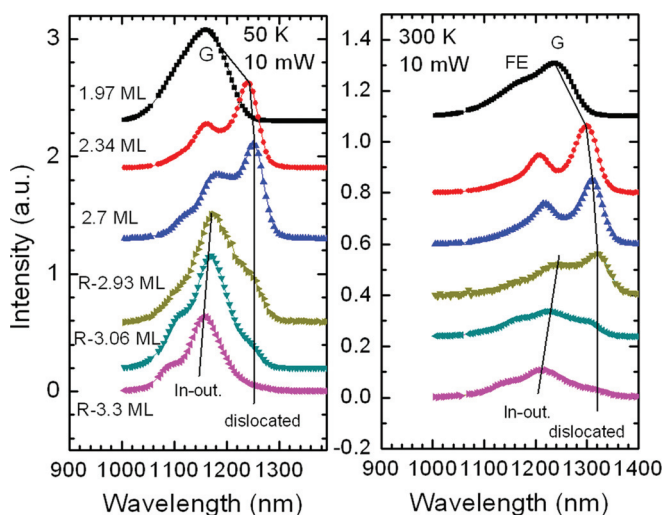


FIG. 1. (Color) (a) The 50 and 300 K PL spectra of the non-relaxed 1.97, 2.34, and 2.7 ML and relaxed 2.93, 3.06, and 3.3 ML QDs. Onset strain relaxation degrades the 1300 nm (at 300 K) transition from the dislocated QDs and generates a blueshifted spectra from the In-outdiffused QDs.

strain relaxation. When temperature is lowered from 300 to 50 K, this blueshifted transition enhances its intensity by a factor of ten and displays well-resolved ground, first- and second-excited spectra Figure 2 illustrates a similar band-filling effect for the 300 K spectra of the non-relaxed 2.7 ML and relaxed R-3.3 ML (R stands for relaxed), normalized to the ground-state peak. With increasing the excitation power, the ground-state emission begins to saturate and subsequently the first and second excited-state emissions increase their intensities. This band-filling effect verifies the blueshifted PL spectra are originated from one dot family. It should be noted that this blueshifted transition is narrower than that of the non-relaxed QDs (the 1.97 ML) emitting at a similar wavelength. Hence, the blueshifted transition is relatively high quality and the associated dot family shall not be severely degraded at the onset relaxation. This dot family cannot be relieved mainly by lattice misfits because the blueshift contradicts a compressive strain reduction, which is expected to decrease the bandgap of the QDs and redshift the wavelength.

To establish the origin for the blueshift, Fig. 3 shows the temperature dependence of the ground-state emission energies for 2.34 and 2.7 ML, and of the blueshifted spectra for R-3.06 and R-3.3 ML, along with the temperature-dependent PL spectra of 2.34 ML and R-3.06 ML in the inset. When temperature is lowered from 300 to 50 K, the transition energy is increased by 45 and 46 meV for 2.34 and 2.7 ML and 51 and 53 meV for R-3.06 ML and R-3.3 ML, respectively. Because the ground-state emission energy and the bandgap of the QDs usually follow similar temperature dependence, this result suggests that the bandgap of the blueshifted dot family has a higher temperature-lowering increment rate than that of the coherent QDs before relaxation. This trend is consistent with a reduction of In content (increase of Ga content) in the QDs because, from the Varshni rule, the bandgap of GaAs (or InGaAs) has a higher temperature-lowering increment rate than that of InAs, and the difference between them is 35 meV from 300 to 50 K. The average increment of 7 meV corresponds to about 20% loss of indium using a linear proportion between the increments of the ground-state emission energy and the bandgap. This estimated In loss is very rough because

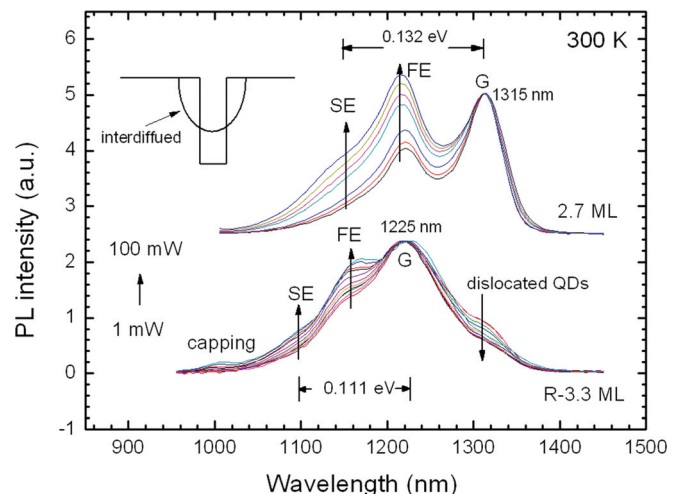


FIG. 2. (Color) 300 K power-dependent band filling for the non-relaxed 2.7 ML and relaxed 3.3 ML QDs, normalized to the ground transition.



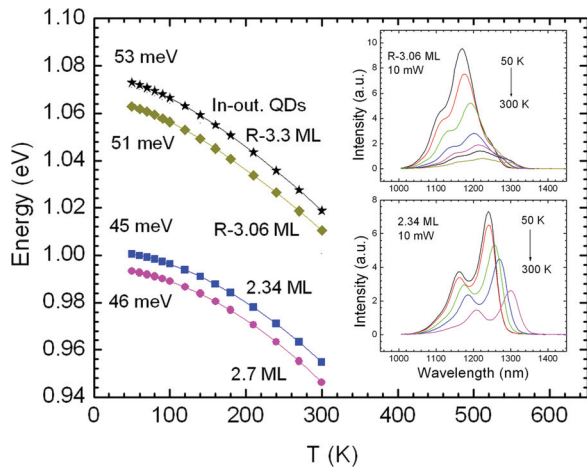


FIG. 3. (Color) Temperature-dependent energy of the ground-state transitions of the non-relaxed 2.34 and 2.7 ML QDs and the In-outdiffused QDs of the relaxed 3.06 and 3.3 ML samples. An obvious increase of the temperature-lowering energy increment can be seen in the relaxed samples, suggesting a reduction of In content in the QDs. The inset shows the temperature-dependent PL spectra of the non-relaxed 2.34 ML and the relaxed R-3.06 ML.

it does not consider a detailed relationship between ground-state emission energy and bandgap. However, the trend is consistent with a composition change from InAs toward InGaAs in the blueshifted dot family, relative to the coherent dots just before relaxation. This result along with the PL blueshift strongly suggests that the blueshifted dot family relieves strain by In/Ga interdiffusion at the onset of relaxation.

Further evidence for In/Ga interdiffusion is provided by a smaller energy separation between the ground and excited emissions, because the occurrence of In/Ga interdiffusion can alter the energy band structure and the excited state would have a wider width (see the simple conduction-band diagram in Fig. 2). As shown in Fig. 2, the abnormal blueshift is 84 meV from 2.7 ML to R-3.3 ML and yet the energy separation between the ground and second-excited emissions is decreased by 21 meV (from 0.132 eV to 0.111 eV). Similarly, the energy separation between the ground and first-excited emissions is decreased in the blueshifted dots, as shown by Fig. 4. The slight decrease from 2.34 to 2.7 ML is due to dot size enlargement before strain relaxation. A sharp drop (about 8 meV) from 2.7 ML to R-3.06 ML is clearly visible. This energy-separation reduction along with the blueshift is consistent with the effect of In/Ga interdiffusion on the energy band structure of the QDs. On the basis of the above analysis, we believe that, at the onset of strain relaxation, a predominant dot family relieves its strain mainly by In/Ga interdiffusion, rather than by lattice misfits, to retain their fine well-resolved PL spectra. We denote this dot family as In-outdiffused QDs. Because of size fluctuation, certain QDs are larger than others to relieve strain by lattice misfits at the critical thickness. With further increasing the InAs coverage, one would expect that all the other QDs would eventually relax by lattice misfits. However, on the basis of the above PL analysis, a predominant dot family relieves its strain by In/Ga interdiffusion even when the InAs coverage is increased to 3.3 ML, which is far beyond the critical thickness. Thus, the relaxation by lattice misfits in

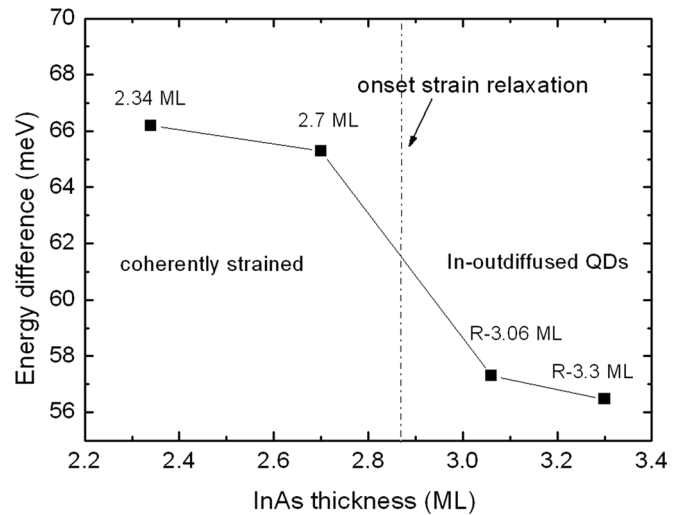


FIG. 4. Energy differences between the ground-state and first excited-state transitions of the non-relaxed 2.34 and 2.7 ML QDs and the In-outdiffused QDs of the relaxed R-3.06 ML and R-3.3 ML. The sharp drop from 2.7 to 3.06 ML supports the occurrence of In/Ga interdiffusion.

certain QDs might affect the adatom migration kinetics and prevent the nearby QDs from strain relaxation by lattice misfits.

## B. TEM analysis

To see the microstructures, Figs. 5(a) and 5(b) show the cross-sectional TEM images of 2.4 ML and R-3.06 ML, respectively. Their statistical distributions of widths and heights are summarized in Fig. 6. The non-relaxed sample shows a uniform trapezium-shaped dot family with an average height of 8.5 nm and an average base width of 20 nm. The relaxed sample shows a similar trapezium-shaped dot family with an average height of 8.8 nm and an average base width of 27 nm, in addition to a few large-size dots with an

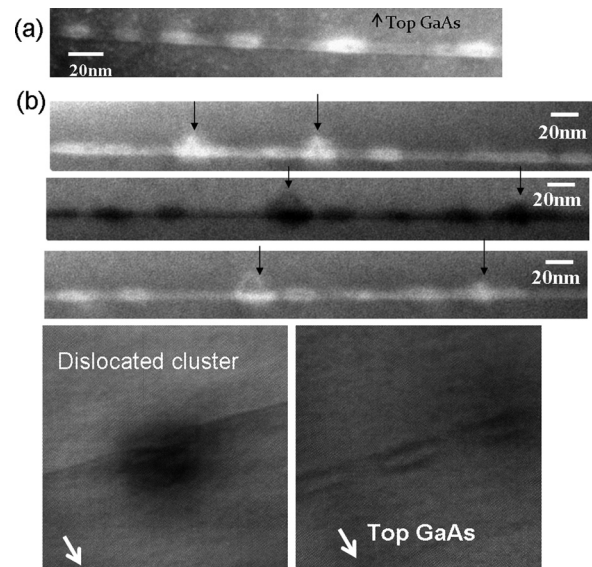


FIG. 5. TEM images of (a) non-relaxed 2.4 ML and (b) relaxed R-3.06 ML. The 3.06 ML sample shows a predominant family of trapezium shaped dots, and a minor substantially large island-like dot family (indicated by arrows).

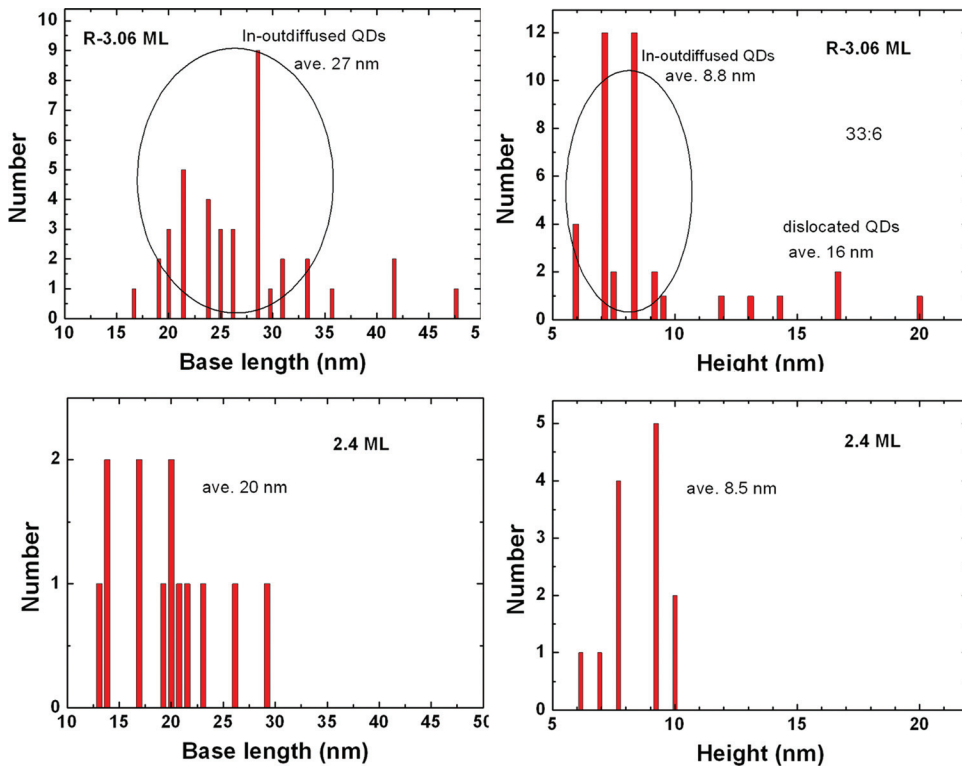


FIG. 6. (Color) Distributions of the widths and heights for the relaxed R-3.06 ML and non-relaxed 2.4 ML samples. The relaxed sample displays two dot families.

average height of 16 nm and an average base width of  $\sim 38$  nm [as indicated by the arrows in Fig. 5(b)]. A typical large-size dot and trapezium dot are shown in the left and right pictures in the bottom of Fig. 5. According to the statistics, the number ratio between the trapezium and the large-size dots is 33:6. In terms of the shape and size, there are two distinctive dot families: a predominant dot family similar to the coherently strained QDs and a minor dot family of large-size dots. To examine lattice misfits, Fig. 7(a) shows the TEM image (the left picture) of a typical trapezium dot in R-3.3 ML and the corresponding Fourier-transformed TEM image (the right picture). The Fourier-transformed TEM reveals no lattice misfits inside the dot but a few misfits under the dot and around the edge, as indicated by circles. This trapezium dot family whose contrast is similar to that of the coherent QDs can be correlated to the In-outdiffused QDs. On the other hand, the large-size dots are associated with lattice misfits. The typical large-size dot in Fig. 7(b) reveals  $\sim 10$  lattice misfits inside the dot and  $\sim 8$  in the neighboring bottom GaAs layer (two in each of the two small loops and four in the large middle loop) right under the QD. These considerable lattice misfits inside the dot can severely degrade the dot and thus the large-size dots are correlated to the dislocated QDs.

On the basis of these TEM observations, we consider the likely onset strain relaxation, as indicated by the schematic diagram in Fig. 8. The InAs deposition produces QDs in Fig. 8(a). The subsequent InGaAs covering can alter the shape of the QDs. Indium atoms can detach from the tops of the QDs and migrate to the base region of the QDs,<sup>24,25</sup> leading to the truncated trapezium-shaped QDs. With the InGaAs covering, the emission wavelength can be extended to about 1300 nm by increasing the dot size and retarding In/Ga interdiffusion. This evolution of growth is generally considered for the coherent QDs. However, when the InAs thickness

exceeds the critical thickness, some QDs are larger than others and are strain relieved by lattice misfits, probably during the InGaAs covering or the initial GaAs covering. These dislocated QDs may attract indium adatoms from the nearby still strained QDs,<sup>18,23</sup> as indicated in Fig. 8(b). This indium detachment leads to In/Ga interdiffusion to relieve strain in the In-outdiffused QDs, yielding the abnormal PL blueshift. The base width extension observed in the In-outdiffused

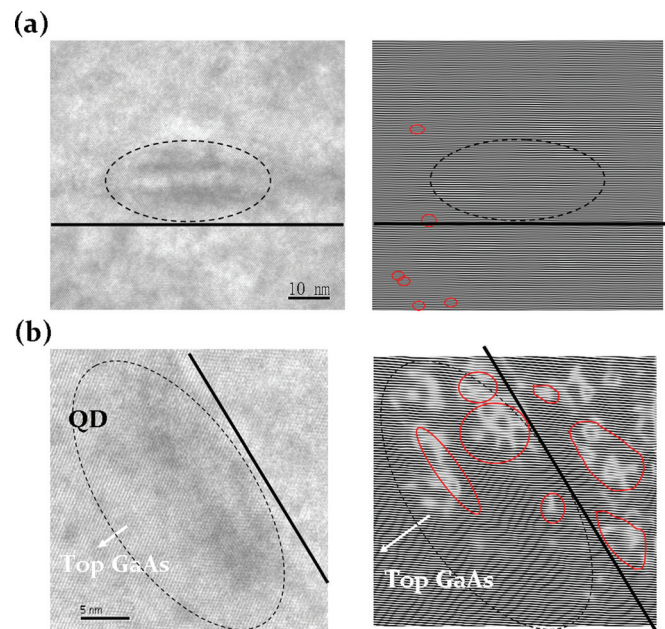


FIG. 7. (Color) Cross sectional TEM pictures of (a) a typical In-outdiffused QD and its Fourier-transformed image and (b) a typical dislocated QD and its Fourier-transformed image in the R-3.3 ML sample. The dislocated dot has a significant number of lattice misfits inside the dot and in the bottom GaAs layer under the dot.

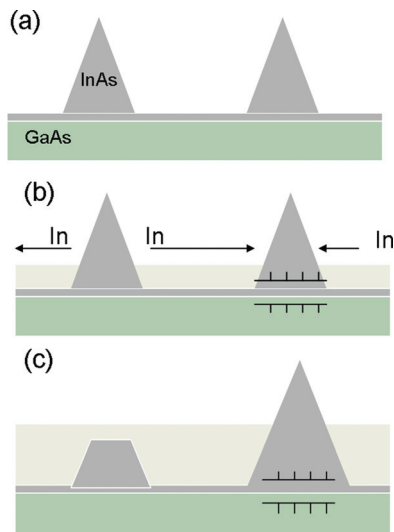


FIG. 8. (Color) Schematic diagram of strain relaxation. (a) Initial growth of the InAs QDs, (b) strain relaxation of the right dot by lattice misfits attracts indium migration from the In-outdiffused dot, and (c) the bimodal strain relaxation.

QDs is characteristic of In/Ga interdiffusion. An increase of the lateral size seen by TEM was previously reported after the InAs QDs were subjected to post-growth thermal annealing and was explained by strain-driven In/Ga interdiffusion.<sup>26</sup> The lack of height (compared with the coherent QDs) is consistent with the deposited indium adatoms not being accumulated in the In-outdiffused QDs, but migrate to the dislocated dots as shown in Fig. 8(c). Therefore, we speculate that the misfit-driven indium migration can detach indium atoms from the In-outdiffused QDs, causing In/Ga interdiffusion to relieve strain.

### C. Post-growth thermal annealing

Figure 9 shows the effect of a post-growth rapid thermal annealing at 650 and 700 °C for one minute on the 300-K PL spectra of the R-3.3 ML. For a clear comparison, the spectra of the 700 °C annealing are shifted up by multiplying a factor of 3. As shown, similar to what is observed in coherent QDs,

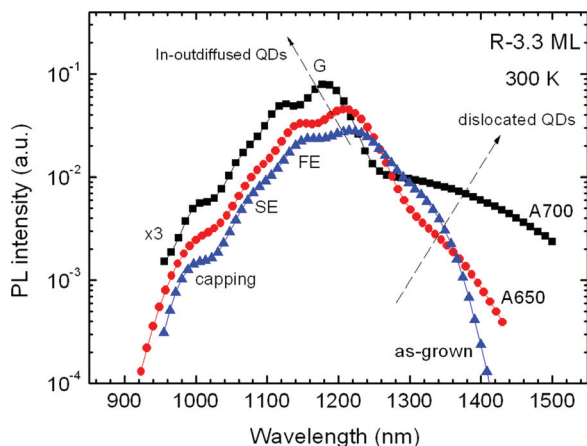


FIG. 9. (Color) 300 K PL spectra of the relaxed R-3.3 ML sample subjected to a post-growth rapid thermal annealing at 650 °C and 700 °C for one minute. Thermal annealing can blueshift the spectra of the In-outdiffused QDs and distend the spectra of the dislocated QDs toward a low-energy side.

thermal annealing can blueshift the transition from the In-outdiffused QDs. Hence, thermal annealing induces In/Ga interdiffusion in the In-outdiffused QDs. Because this interdiffusion is driven by strain, this result suggests retention of considerable strain in the In-outdiffused QDs before thermal annealing. On the other hand, thermal annealing can shift the transition from the dislocated QDs toward low energy, and generate a tail up to 1500 nm after 700 °C annealing. Hence, the dislocated QDs undergo strain relief not by In/Ga interdiffusion but by introducing more dislocations to decrease the bandgap of the QDs. Note that the opposite PL shift is consistent with the different nature of strain distribution in the two dot families, supporting the claimed bimodal strain relaxation.

Relative to annealing at 650 °C, annealing at 700 °C can produce a low-energy tail up to 1500 nm. To understand this large change, Fig. 10 shows the DLTS spectra of the 650 °C and 700 °C annealing samples, measured for different voltage sweepings. The spectra of the 650 °C annealing (shifted up for clarity) reveal a misfit-related trap at  $\sim 0.35$  eV near the QD region (approximately  $-2/-3.5$  V) while the top GaAs layer is almost defect-free (with a very weak intensity of the misfit-related trap). These spectra are similar to those observed in the as-grown sample.<sup>20</sup> This result suggests that annealing at 650 °C does not significantly introduce more dislocations to relieve strain and the redshift is not appreciable. On the other hand, annealing at 700 °C significantly alters the DLTS spectra. A prominent trap at 0.61 eV ( $\sigma = 9.1 \times 10^{-15}$  cm<sup>2</sup>) with significant intensity is detected in the top GaAs layer with an emission time two orders of magnitude longer than that of the misfit trap. This trap displays a signature of threading dislocations from a comparison with previously reported Arrhenius plots.<sup>27,28</sup> The intensity of this trap shows no saturation even when the filling pulse duration time is increased to 100 ms, characteristic of a threading-dislocation trap, which shall exhibit a logarithmic function with filling pulse duration time and is reflective of Coulombic repulsion of the carriers captured at the traps along the linearly arrayed dislocation lines.<sup>27</sup> Hence, thermal annealing at 700 °C provides sufficient thermal energy for the generation of threading dislocations in the

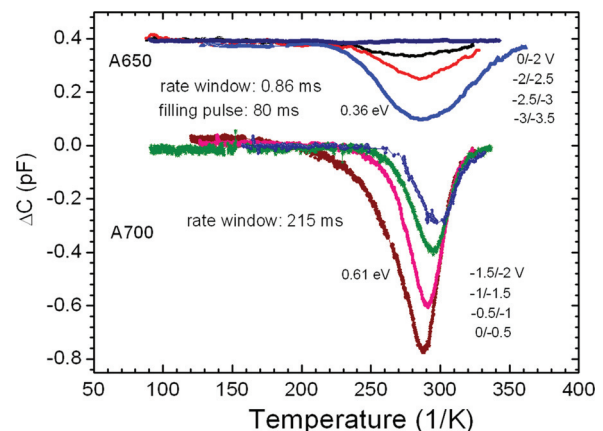


FIG. 10. (Color) DLTS spectra of the relaxed 3.3 ML sample after 650 °C and 700 °C annealing. The spectra of 650 °C annealing display the misfit trap near the QD region (at approximately  $-3/-3.5$  V) while the spectra of 700 °C annealing reveal a threading-dislocation trap at 0.61 eV in the top GaAs layer.



top GaAs, layer probably by the gliding process through the lattice misfits near the QDs due to elastic acting as a shear stress.<sup>28</sup> The generation of these threading dislocations can cause significant strain relieving in the QDs to decrease the bandgap of the QDs, leading to the redshift toward 1500 nm. Therefore, a pure strain relieving by lattice misfits (without In/Ga interdiffusion) near the QDs does not significantly relieve strain to decrease the bandgap, and only by the generation of threading dislocations in the GaAs layer can strain significantly be relieved to reduce the bandgap for observing an apparent redshift. This can explain why the dislocated dots emit a wavelength similar as that of the coherent dots before relaxation, as shown in Fig. 1.

#### D. C-V spectra

The lattice misfits at  $\sim 0.35$  eV (relative to the GaAs conduction-band edge) are effective electron traps that can compensate the ionized impurity in the bottom GaAs layer and cause drastic carrier depletion.<sup>29</sup> This compensation extends to the regions under the In-outdiffused QDs, forming a completely connected depletion layer in the bottom GaAs layer. This can be seen by the 300 K apparent-carrier concentration profiling (converted from C-V spectra) of the R-3.3 ML sample in Fig. 11. Although the top GaAs layer displays a normal depletion near the QDs with a designed background  $N_D = 9 \times 10^{16} \text{ cm}^{-3}$ , the bottom GaAs layer displays a nearly double depletion width. On the basis of a simple Schottky depletion model  $V = (q/2\epsilon)N_D L^2$ , a double depletion width would require a decrease of the background concentration from  $9 \times 10^{16} \text{ cm}^{-3}$  to  $2.25 \times 10^{16} \text{ cm}^{-3}$ , yielding an average trapped electron concentration  $N_t = 6.75 \times 10^{16} \text{ cm}^{-3}$ . Detailed differential capacitance analysis has yielded a similar concentration.<sup>29</sup> As shown in Fig. 11, the C-V spectra show a sharp electron-confinement peak related to the In-outdiffused QDs and the drastic carrier depletion. Further decreasing reverse voltage can push down the Fermi level to intersect with the misfit-related traps, and more reverse voltage is needed for the Fermi level to sweep out the trapped

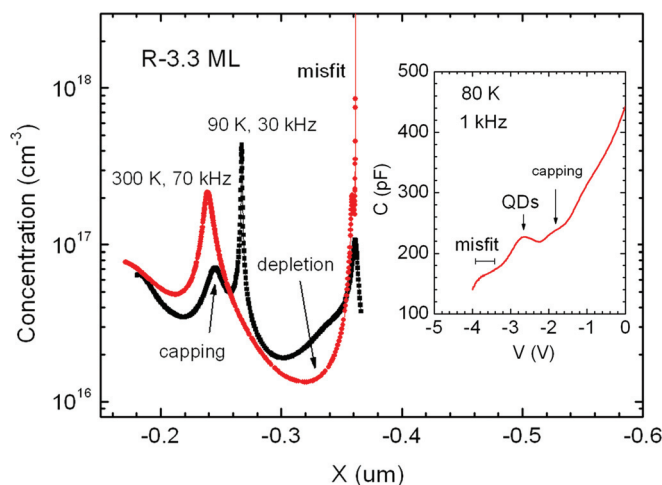


FIG. 11. (Color) Apparent-carrier concentrations of the R-3.3 ML sample, measured at 90 K, 30 kHz, and 300 K, 70 kHz, respectively. These concentrations are converted from C-V spectra, as is the one measured at 80 K and 1 kHz in the inset.

electrons and yield the misfit-related C-V plateau (from  $-3.5$  to  $-4$  V), as shown in the inset of Fig. 11. In order to sweep out the trapped electrons, the edge of the depletion region needs to move a width of  $0.358 - 0.328 = 0.03 \mu\text{m}$ , determined from  $C = 175$  to  $160$  pF in the misfit plateau. This width and the trapped electron concentration ( $6.75 \times 10^{16} \text{ cm}^{-3}$ ) yields trapped electrons of  $2 \times 10^{11} \text{ cm}^{-2}$ . This is about one order of magnitude higher than the QD density (about  $3 \times 10^{10} \text{ cm}^{-2}$ ) and is comparable to the total electrons confined in the In-outdiffused QDs.

Because the drastically depleted region can suppress tunneling, electrons in the In-outdiffused QDs need a substantial time to emit to the bottom GaAs layer. The long emission time can be easily measured by the resolvable frequency dispersion in Fig. 12. To obtain the electronic band, we use the high-frequency capacitance at 100 kHz (where the QD electrons cannot follow to be modulated) to obtain the depletion-region width  $L$ , and the confinement energy  $E$  (relative to the GaAs conduction-band edge) of the Fermi-level probed electrons in the QDs, from a simple Schottky depletion model,  $E = (q/2\epsilon)N_D(L - 0.2)^2 + (kT/q)\ln(N_c/N_D)$ , where  $N_D$  is the compensated concentration in the bottom GaAs layer,  $0.2 \mu\text{m}$  is the distance of the QD layer from the surface and  $N_c$  is the effective density of states in the GaAs conduction band. Thus, each reverse bias can be converted to an  $E$ . The corresponding electron density of states in the QDs (at this  $E$ ),  $C_Q$ , can be obtained from the low-frequency capacitance (at 3 kHz) using  $C_L = \frac{(C_1 + C_Q)C_2}{(C_1 + C_Q) + C_2}$ , where  $C_1 = \epsilon/(L - 0.2)$  and  $C_2 = \epsilon/0.2$  are the geometric capacitance from the QD layer to the edge of the depletion region and from the sample surface to the QD layer, respectively.<sup>30</sup> The obtained electronic band is shown in the inset of Fig. 12, which can be correlated to the capping layer, first-excited, and ground states of the In-outdiffused QDs and dislocated QDs by a comparison with the PL spectra. The dislocated QDs peaked at 0.3 eV are 47 meV below the ground state of the In-outdiffused QDs. Comparing with the difference of 71 meV in the 300 K PL spectra (1.019 and 0.948 eV from the In-outdiffused and dislocated QDs, respectively), the ratio for the band-offsets between electrons and holes is 6.6:3.4, a value close to that

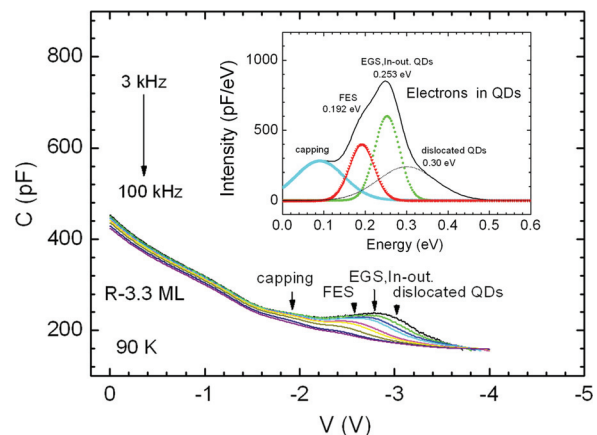


FIG. 12. (Color) 90 K C-V spectra of the R-3.3 ML sample, which shows the electron confinements of the capping layer, the first-excited and ground states of the In-outdiffused QDs and the dislocated QDs, as illustrated by the converted electronic band in the inset.

previously reported.<sup>31</sup> Hence, the electronic band displays a bimodal structure. Also, the C-V plateau at around  $-3$  V can be attributed to the electrons in the In-outdiffused QDs even though its emission time is five orders of magnitude longer than that of the coherent QDs before relaxation. This analysis explains the co-existence of strong dot-carrier confinement and enormous misfit-related traps. The elongation of the emission time is due to the alteration of the electron emission process in the In-outdiffused QDs.

#### IV. CONCLUSIONS

This work presents a detailed study of onset strain relaxation in InAs QDs. Evidence is presented to show a bimodal strain relaxation in which a minor dot family is relaxed by lattice misfits and a predominant dot family is relaxed by In/Ga interdiffusion. This bimodal strain relaxation is supported by TEM pictures, which display a predominant family of trapezium shaped dots, similar to those observed in the coherent QDs, and a minor dot family of large-size dislocated dots. A likely mode of strain relaxation is discussed to explain the observed PL blueshift. Thermal annealing can produce opposite wavelength shift in the two dot families. This bimodal strain relaxation can explain the elongated electron emission time in the relaxed QD samples.

#### ACKNOWLEDGMENTS

The authors would like to thank the National Science Council of the Republic of China, Taiwan (Contract No. NSC-97-2112-M-009-014-MY3) and for financially supporting this research. Dr. J. Y. Chi and R. S. Hsiao are commended for preparing the samples.

- <sup>1</sup>F. Heinrichsdorff, M. H. Mao, N. Kirstaedter, A. Krost, and D. Bimberg, *Appl. Phys. Lett.* **71**, 22 (1997).
- <sup>2</sup>D. J. Eaglesham and M. Cerullo, *Phys. Rev. Lett.* **64**, 1943 (1990).
- <sup>3</sup>D. Leonard, K. Pond, and P. M. Petroff, *Phys. Rev. B* **50**, 11683 (1994).
- <sup>4</sup>J. M. Moison, F. Houzay, F. Barthe, and L. Leprince, *Appl. Phys. Lett.* **64**, 196 (1994).
- <sup>5</sup>C. W. Snyder, J. F. Mansfield, and B. G. Orr, *Phys. Rev. B* **46**, 551 (1992).
- <sup>6</sup>H. Shoji, K. Mukai, N. Ohtsuka, M. Sugawara, T. Uchida, and H. Ishikawa, *IEEE Photonics Technol. Lett.* **7**, 1385 (1995).
- <sup>7</sup>G. Yusa and H. Sakaki, *Electron. Lett.* **32**, 491 (1996).

- <sup>8</sup>J. C. Campbell, D. L. Huffaker, H. Deng, and D. G. Deppe, *Electron. Lett.* **33**, 1337 (1997).
- <sup>9</sup>C. M. A. Kapteyn, F. Heinrichsdorff, O. Stier, R. Heitz, M. Grundmann, and P. Werner, *Phys. Rev. B* **60**, 14265 (1999).
- <sup>10</sup>P. N. Brunkov, A. Patane, A. Levin, L. Eaves, P. C. Main, Y. G. Musikhin, B. V. Volovik, A. E. Zhukov, V. M. Ustinov, and S. G. Konnikov, *Phys. Rev. B* **65**, 085326 (2002).
- <sup>11</sup>J. M. Garcia, J. P. Silveira, and F. Briones, *Appl. Phys. Lett.* **77**, 409 (2000).
- <sup>12</sup>X. Letartre, D. Stievenard, and M. Lanoo, *J. Appl. Phys.* **69**, 7336 (1991).
- <sup>13</sup>H. Drexler, D. Leonard, W. Hansen, J. P. Kotthaus, and P. M. Petroff, *Phys. Rev. Lett.* **73**, 2252 (1994).
- <sup>14</sup>S. Sauvage, P. Boucaud, F. H. Julien, J.-M. Gerard, and J.-Y. Marzin, *J. Appl. Phys.* **82**, 3396 (1997).
- <sup>15</sup>H. L. Wang, F. H. Yang, S. L. Feng, H. J. Zhu, D. Ning, H. Wang, and X. D. Wang, *Phys. Rev. B* **61**, 5530 (2000).
- <sup>16</sup>J. S. Wang, J. F. Chen, J. L. Huang, P. Y. Wang, and X. J. Guo, *Appl. Phys. Lett.* **77**, 3027 (2000).
- <sup>17</sup>J. F. Chen and J. S. Wang, *J. Appl. Phys.* **102**, 043705 (2007).
- <sup>18</sup>N. A. Cherkshin, M. V. Marksimov, A. G. Makarov, V. A. Shehukin, V. M. Ustinov, N. V. Lukovskaya, Y. G. Musikhin, G. E. Cirilin, N. A. Bert, Z. I. Alferov, N. N. Ledentsov, and D. Bimberg, *Semiconductors* **37**, 861 (2003).
- <sup>19</sup>J. F. Chen, R. S. Hsiao, Y. P. Chen, J. S. Wang, and J. Y. Chi, *Appl. Phys. Lett.* **87**, 141911 (2005).
- <sup>20</sup>J. F. Chen, Y. Z. Wang, C. H. Chiang, R. S. Hsiao, Y. H. Wu, L. Chang, J. S. Wang, T. W. Chi, and J. Y. Chi, *Nanotechnology* **18**, 355401 (2007).
- <sup>21</sup>C. W. Snyder, B. G. Orr, D. Kessler, and L. M. Sander, *Phys. Rev. Lett.* **66**, 3032 (1991).
- <sup>22</sup>M. V. Maximov, A. F. Tsatsulnikov, B. V. Volovik, D. S. Sizov, Y. M. Shernyakov, I. N. Kauander, A. E. Zhukov, A. R. Kovsh, S. S. Mikhlin, V. M. Ustinov, Z. I. Alferov, R. Heitz, V. A. Shchukin, N. N. Ledentsov, D. Bimberg, Y. G. Musikhin, and W. Neumann, *Phys. Rev. B* **62**, 16671 (2000).
- <sup>23</sup>T. S. Shamirzaev, A. M. Gilinsky, A. K. Kalagin, A. I. Toropov, A. K. Gutakovski, and K. S. Zhuravlev, *Semicond. Sci. Technol.* **21**, 527 (2006).
- <sup>24</sup>N. N. Ledentsov, J. Bohrer, D. Bimberg, I. V. Kochnev, M. V. Maximov, P. S. Kopev, Z. I. Alferov, A. O. Kosogov, S. S. Ruvimov, P. Werner, and U. Gosele, *Appl. Phys. Lett.* **69**, 1095 (1996).
- <sup>25</sup>F. Ferdos, S. Wang, Y. Wei, A. Larsson, M. Sadeghi, and Q. Zhao, *Appl. Phys. Lett.* **81**, 1195 (2002).
- <sup>26</sup>A. Babinski, J. Jasinski, R. Bozek, A. Szepielow, and J. M. Baranowski, *Appl. Phys. Lett.* **79**, 2576 (2001).
- <sup>27</sup>T. Wosinski, *J. Appl. Phys.* **65**, 1566 (1989).
- <sup>28</sup>Y. Uchida, H. Kakibayashi, and S. Goto, *J. Appl. Phys.* **74**, 6720 (1993).
- <sup>29</sup>F. Chen, Ross C. C. Chen, C. H. Chiang, M. C. Hsieh, Y. C. Chang, and Y. F. Chen, *J. Appl. Phys.* **108**, 063705 (2010).
- <sup>30</sup>J. F. Chen, Ross C. C. Chen, C. H. Chiang, Y. F. Chen, Y. H. Wu, and L. Chang, *Appl. Phys. Lett.* **97**, 092110 (2010).
- <sup>31</sup>S. D. Lin, V. V. Ilchenko, V. V. Marin, K. Y. Panarian, A. A. Buyanin, and O. V. Tretyak, *Appl. Phys. Lett.* **93**, 103103 (2008).